

11:58:11

OCA PAD AMENDMENT - PROJECT HEADER INFORMATION

10/22/91

Active

Project #: E-25-625

Cost share #:

Rev #: 1

Center # : 10/24-6-R7156-0A0

Center shr #:

OCA file #:

Contract#: A71454

Mod #: ONE (1)

Work type : RES

Prime # : NAS8-36200

Document : CONT

Contract entity: GTRC

Subprojects ? : N

CFDA: N/A

Main project #:

PE #: N/A

Project unit:

MECH ENGR

Unit code: 02.010.126

Project director(s):

ERNST H A

MECH ENGR

(404)894-3074

Sponsor/division names: MARTIN MARIETTA CORP

/

Sponsor/division codes: 212

/ 009

Award period: 910308 to 911231 (performance) 911231 (reports)

Sponsor amount

New this change

Total to date

Contract value

0.00

85,000.00

Funded

0.00

85,000.00

Cost sharing amount

0.00

Does subcontracting plan apply ? : N

Title: RESISTANCE CURVE ANALYSIS OF SURFACE CRACKS

PROJECT ADMINISTRATION DATA

OCA contact: E. Faith Gleason

894-4820

Sponsor technical contact

Sponsor issuing office

NORMAN ELFER
(504)257-3162

STEVE CROW, MAIL NO. 3830
(504)257-1604

MARTIN MARIETTA CORP.
MAIL STOP NO. 3573
P.O. BOX 29304
NEW ORLEANS, LA 70189

MARTIN MARIETTA CORP
P.O. BOX 29304
NEW ORLEANS, LA 70189

Security class (U,C,S,TS) : U

Defense priority rating :

Equipment title vests with:

N/A

Sponsor

ONR resident rep. is ACO (Y/N): N

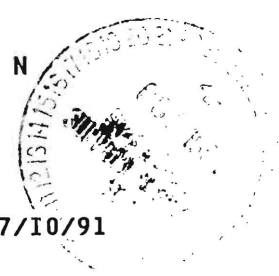
N/A supplemental sheet

GIT

Administrative comments -

* AMENDMENT NO. 1 REVISES THE STATEMENT OF WORK, IN ACCORDANCE WITH THE 7/10/91
REVISION, AND EXTENDS THE PROJECT TO 12/31/91.

2



5K682-2

GEORGIA INSTITUTE OF TECHNOLOGY
OFFICE OF CONTRACT ADMINISTRATION

NOTICE OF PROJECT CLOSEOUT

Closeout Notice Date 04/02/92

Project No. E-25-625_____ Center No. 10/24-6-R7156-0A0_
Project Director ERNST H A_____ School/Lab MECH ENGR_____
Sponsor MARTIN MARIETTA CORP/_____
Contract/Grant No. A71454_____ Contract Entity GTRC
Prime Contract No. NAS8-36200_____
Title RESISTANCE CURVE ANALYSIS OF SURFACE CRACKS_____
Effective Completion Date 911231 (Performance) 911231 (Reports)

Closeout Actions Required:	Y/N	Date Submitted
Final Invoice or Copy of Final Invoice	Y	_____
Final Report of Inventions and/or Subcontracts	Y	_____
Government Property Inventory & Related Certificate	N	_____
Classified Material Certificate	N	_____
Release and Assignment	N	_____
Other _____	N	_____
Comments_____		

Subproject Under Main Project No. _____

Continues Project No. _____

Distribution Required:

Project Director	Y
Administrative Network Representative	Y
GTRI Accounting/Grants and Contracts	Y
Procurement/Supply Services	Y
Research Property Management	Y
Research Security Services	N
Reports Coordinator (OCA)	Y
GTRC	Y
Project File	Y
Other _____	N
_____	N

NOTE: Final Patent Questionnaire sent to PDPI.

RESISTANCE CURVE ANALYSIS OF SURFACE CRACKS

CONTRACT SC-273276

ANNUAL REPORT - FISCAL YEAR 1991

Prepared for:

Norman Elfer, Project Monitor

*Martin Marietta Manned Space Systems
P.O.Box 29304
New Orleans, LA 70189*

Prepared by:

Prof. Hugo A. Ernst

*School of Mechanical Engineering
Georgia Institute of Technology
Atlanta, GA 30332*

October 1991

INDEX

1. Introduction

- 1.1 Background
- 1.2 The Program
- 1.3 This Report

2. Analytical Studies

- 2.1 Critical Review of Existing Methodology
 - R-Curve Data
 - Calibration Curves
 - J Estimations

2.2 Analysis

2.3 Results

3. Constraint Effects

4. Data Generation

5. Conclusions

6. References

7. Tables

8. Figures

1. INTRODUCTION

1.1 Background

Reliable analysis is necessary for the disposition of surface flaws in External Tank (ET) hardware. Martin Marietta Manned Space Systems (MM) is currently using a conservative approach to analyze surface flaws in 2219 Al. This procedure is very conservative and has not been empirically verified for other materials.

A database expansion to include flaws with two proof tests, with combined tension and bending loads, and materials such as (but not limited to) 21-6-9 is underway. Time-consuming testing and analysis must be performed upon test completion to determine if the current surface flaw analysis procedure is applicable to these configurations and materials.

1.2 The program

The objective of this research program was to perform the R-Curve testing and analysis of test data.

The Scope of the program, as provided by MM in the Statement of Work, is detailed in the following tasks.

Task 1. Preliminary Analytical Studies of Existing Methodology

Task 1 work involves a study and evaluation of existing analysis methodology. The following evaluations should be applied to various experimental data.

- a) The adequacy of the J values used in R-Curve methodology should be verified. This study includes developing a method to estimate J as a function of crack front position.
- b) The evolution of the crack front needs to be studied. Little data regarding crack front geometry exists in the current database. A better understanding of crack geometry evolution would lead to a more accurate analysis.

Task 2. Characterization of Constraint

Characterization of crack front constraint should be studied. It is theorized that this constraint varies with crack position and is a factor in crack front geometry.

Task 3. Development of Methodology

A method of using the experimental results in accurately predicting crack growth must be established.

Task 4. Data Generation

Experimental data for materials other than 2219 Al should be generated. The Equivalent Energy R-Curve Methodology should be applied to this data to determine if the R-Curve methodology currently used at MM is applicable to other materials. MM will supply 21-6-9 test pannels for use in Task 4.

Task 5. Non-proportional Loading

The condition of combined tension and bending is neither well understood nor well documented. This condition is experienced by various ET flight hardware and needs to be better understood. Testing of J parameters needs to be performed to determine the application that is best suited to model ET hardware.

1.3 This Report

The program had originally a period of performance from 3/8/91 through 9/30/91. Georgia Tech requested, and was granted, a no-cost extension of the program until 12/30/91. Thus this is a Status Report, reflecting the progres made to date. The Final Report will be issued at a corresponding later date.

During these first six months of performance, efforts have been principally devoted to Task 1, 2 and 4, according to the original plan. Due to their intrinsic nature, Tasks 3 and 5 cannot be started until the others are completed.

2. ANALYTICAL STUDIES

2.1 Critical Review of Existing Methodology

R-Curve Data

It was principally D.E. McCabe, [1-3], who developed different aspect of a program to assess the behavior and predict the crack growth characteristics of surface flaws in 2219-T87 TIG material. The most salient features of his multi-year project are summarized below:

- * The program was devoted to 2219-TIG welds.
- * R curves were developed for planar specimens of different geometries.
- * R curves were developed for surface cracks. Method of analysis considers a) average crack length determined from change in the compliance corresponding to semielliptical defects, b) J is obtained by scaling up the value of G with a factor equal to the ratio of plastic to elastic area, i.e. it is based on equivalent energy (EE) concepts, or more precisely assumes that $\eta_{el} = \eta_{pl}$.
- * The former R curves compare well with those from CT specimens.
- * Calibration curves were obtained for surface cracks in terms of load-crack mouth displacement, P-v. The curves were normalized in Key Curve format. Expressions for J were obtained.
- * Calibration curves were obtained for combined bending-tension loading, proportionally applied. Curves were normalized in Key Curve format. Expressions for J were obtained.
- * R curve data were generated for combined loading cases. The agreement with two dimensional specimen data was not always good.

It was concluded that although the approaches used show promise it is still mandatory to devote significant efforts to improve several areas before the methodology could be safely applied. Specifically, the following areas were identified:

- a) The adequacy of the J values obtained using Equivalent Energy methods must be validated. Particular for the case of combined bending and tension. Crack growth needs to be included in the procedure. Method needs to be developed to estimate the value of J as a function of position along the crack front.
- b) The change in compliance gives one average value of crack length. A method needs to be developed to get more information about the evolution of the crack shape.
- c) Methodology has to be developed to better characterize crack growth in the irregular mushroom type of crack shape. So far only growth in two directions were calculated one parallel to the plate surface at the point of largest crack extension and one at the deepest point. Presumably there are better ways of identifying corresponding pairs of initial and final points along the crack front to define crack growth as a function of position.

Key Curves or Calibration Curves

As part of the mentioned program, McCabe obtained load vs plastic displacement, ($P-v_{pl}$), records for different constant crack lengths, or calibration curves, for SCT specimens of the mentioned 2219-T87 Tig material. The experimental program included plate thicknesses of 1/4 and 1/2 in.

These calibrations curves were normalized in a Key Curve format, by McCabe [3] and Ernst [4]. The general expression obtained was:

$$\sigma = (P/Wt) = \beta_o (a/c)^p (a/t)^m (v_{pl}/t)^N \quad (1)$$

where:

σ	stress
N	= 1/n, hardening exponent
P	load
W	specimen width
t	specimen thickness
a	crack depth
c	half of the crack surface length
v_{pl}	plastic part of the displacement

In the case of the 1/2 " thick plate, the material constants were, [3]:

$$\begin{aligned}\beta_0 &= 78,534 \text{ psi} \\ p &= 0.138 \\ m &= -0.224 \\ N &= 0.294 = 1 / 3.401\end{aligned}$$

For the 1/4 " plate the constants were, [4]:

$$\begin{aligned}\beta_0 &= 60,930 \text{ psi} \\ p &= 0.120 \\ m &= -0.270 \\ N &= 0.302 = 1/3.311\end{aligned}$$

J Estimations.

The J-integral can be defined as the difference in potential energy of two cracked bodies subjected to the same loading history, differing only in their crack length by a small amount, per unit cracked area difference, [5]. In the particular case of planar specimens the crack is characterized by one length parameter, i.e. a ; the incremental cracked area is simply $dA = B da$, where B is the specimen thickness.

On the other hand, as pointed out by Ernst [4], when two parameters are needed to characterize the crack, i.e. a and c in our case of 3D cracks, global values of J are linked to the particular way in which the virtual crack extension is taken.

In that study, three cases were considered: 1) increasing c , keeping a constant, 2) increasing a keeping, c constant, and 3) increasing both a and c to keep a/c constant. It was shown that for the three cases the expressions for the plastic part of J , J_{pl} , are of a similar form, differing only in a coefficient called η_{pl} , [6-7]. These values are global J_{pl} , i.e. $J_{plG,a}$; $J_{plG,c}$; and $J_{plG,a/c}$ respectively.

The expressions for J_{pl} , as a function of crack shape parameters and area under the $P-v_{pl}$ record, as a function of crack shape parameters and v_{pl} , and as a function of crack shape parameters and P are given by the following equations:

$$\begin{aligned}
J_{pl} &= \frac{\eta_{pl}}{(\pi/2) a c} \int_0^{v_{pl}} P dv_{pl} \\
&= \frac{\eta_{pl}}{(\pi/2) a c} \frac{W t^2}{(N+1)} \beta_o (a/c)^p (a/t)^m (v_{pl}/t)^{N+1} \\
&= \beta_o \frac{\eta_{pl}}{(\pi/2) a c} \frac{W t^2}{(N+1)} \left[\frac{a}{c} \right]^{-p/N} \left[\frac{a}{t} \right]^{-m/N} \left[\frac{P}{W t \beta_o} \right]^{(1+N)/N}
\end{aligned} \tag{2}$$

Values of η_{pl} are shown below for the three different cases studied:

Constant	η_{pl} expression	η_{pl} value $t = 0.25''$
a	-(p+m)/2	0.075
c	p/2	0.060
a/c	-m/2	0.135

Note that the values of η_{pl} are independent of the a/c and a/t ratio.

Although these developments are significant, it is important to emphasize here, that there are two problematic points that need to be resolved:

- * It is not clear which one of the three methods of incrementing the cracked area, i.e. constant a, c or a/c, gives a result for J that is more appropriate or significant to this problem.
- * Values of J obtained with these approaches are 'global values'. There is still a need to obtain J as a function of position along the crack front.

2.2 Analysis

Normalization Scheme

The incremental energy, δE , needed to grow a crack from an initial to a final shape differentially close to the first one, normalized by the difference in crack area δA , can be expressed as:

$$\frac{\delta E}{\delta A} = \frac{1}{\delta A} \int_0^l J \, ds \, dn \quad (3)$$

where J is a function of the position on the front; ds represents a differential element of arc along the crack front; dn represents the distance, along the normal direction, from the initial to the final crack front, and the integral is taken along the full perimeter of the crack front, l .

At the same time, the quantity δE is connected to the differential work done by the external forces, δW , and the additional strain energy, δU , absorbed by the body as

$$\delta W / \delta A = (\delta E + \delta U) / \delta A \quad (4)$$

Obviously the incremental quantities δW and δU can be obtained from global quantities, i.e. the load-displacement characteristics. In the special cases of growth at constant displacement, $\delta W = 0$ and the above equation gives,

$$\delta E / \delta A = - \delta U / \delta A \quad \text{at constant } v$$

$$= - \frac{d}{dA} \int_0^v P \, dv \quad (5)$$

This is a general result independent of the initial and final shapes. Let us now consider the special case of a semielliptical crack with aspect ratio a/c , growing to a final shape that is also semi-elliptical and with the same a/c ratio. For this case, the expression for ds , dl and dA , [4], are:

$$\begin{aligned} ds &= \left[(c \cos \phi)^2 + (a \sin \phi)^2 \right]^{1/2} d\phi \\ dn &= 2 c da \left[(c \cos \phi)^2 + (a \sin \phi)^2 \right]^{-1/2} \\ \delta A &= \pi c da \end{aligned} \quad (6)$$

where ϕ is the elliptical angle as shown in Fig. 1. Correspondingly, the energy rate $\delta E/\delta A$ is given by,

$$\delta E / \delta A = \frac{2}{\pi} \int_0^{\pi/2} J d\phi = J_{ave} = J_{G, a/c} \quad (7)$$

where J_{ave} and $J_{G, a/c}$ represent respectively, the linear average along the crack front and the global value of J , obtained by taking the incremental growth at $a/c=\text{constant}$, as discussed above.

This is a result of the most significant importance: 1) the linear average of J along the front is numerically equal to the global J obtained by taking a growth step with $a/c=\text{constant}$ (and not any other), 2) the result is independent of the material behavior, i.e. linear or non-linear elastic. Thus, it applies to G , J_{pl} or total J .

This result can be also used as a normalization requirement: "The linear average of J (or G) along the crack front has to be numerically equal to the difference in strain energy of two bodies with the same a/c and differentially different a/t ratio, per unit crack area difference." In what follows, the importance of this result will become more apparent.

Estimation of J as a Function of Position

Several authors, [8-9], have demonstrated that the distribution of J_{pl} along the crack front follows that of G , for moderate amounts of plastic deformation. What sometimes is not so clear is how to find the coefficient of proportionality between the two distributions as a function of a/c , a/t , material deformation properties and applied deformation. This is the objective of this section.

Let us assume that J_{pl} and G , as functions of elliptical angle ϕ , are linearly related:

$$J_{pl}(\phi) = k G(\phi) \quad (8)$$

$$J = G + J_{pl} = G(1 + k) \quad (9)$$

Correspondingly the linear averages along the crack front will be also linearly related:

$$\frac{2}{\pi} \int_0^{\pi/2} J_{pl} d\phi = \frac{2}{\pi} k \int_0^{\pi/2} G d\phi = J_{plG, a/c} \quad (10)$$

and as a result the proportionality factor k can be obtained as:

$$k = \frac{J_{plG, a/c}}{G_{ave}} \quad (11)$$

It is convenient to define a coefficient D independent of applied stress as:

$$D = \frac{k}{\sigma^{(n+1)}} \quad (12)$$

where n is the hardening exponent ($1 < n < \infty$). Using Eqs. (2), (11) and (12) D is:

$$D = \frac{0.224 \ n \ W}{\pi \ (n+1) \ \beta_o^n \ (G_{ave} / \sigma^2)} \ (a/c)^{(1-pn)} \ (a/t)^{-(2+mn)} \quad (13)$$

The value of J_{pl} as a function of position is then

$$J_{pl}(\phi) = D \ \sigma^{n-1} \ G(\phi) \quad (14)$$

$$J(\phi) = G(\phi) \ (1 + D \ \sigma^{n-1}) \quad (15)$$

2.3 Results

Normalized values of G , [10], $G_n = (E G t / \sigma^2)$ as a function of angle ϕ are shown in Figs. 2-4 for $a/c = 0.6$; 1.0; and 2.0 and a/t values of 0.35; 0.55; and 0.75. It can be noted that for $a/c=0.6$ the value of G_n is higher at the deepest point ($\phi=\pi/2$) than at the surface ($\phi=0$). Whereas for $a/c = 1$ and 2, the converse is true. Average values of G_n , G_{nave} appear in Table 1.

Using the scheme developed above values of total J as a function of angle ϕ were calculated for different conditions and load levels. The results are shown in Figs. 5-7. Values of the coefficient D appear in Table 2.

3. CONSTRAINT EFFECTS

It is well known that constraint varies along the crack front. Moreover, it is also commonly accepted that the reason for the complex shape of the growing crack is due to the difference in constraint, and as a result different resistance to crack extension, along the crack front.

Preliminary studies have been conducted in this area. The literature has been reviewed and tentatively candidate constraint parameters have been identified. Among others, the T , [11], and Q , [12], stress factors, and the ratio of hydrostatic to Von Mises stress, h , [13], seem to show promise. Work is under way to implement their use in this program.

Other parameters are also being evaluated. Specifically, it has been shown that the second order term in the series expansion of the crack opening displacement profile is proportional to the partial derivative of K with respect to crack length at constant load, [14]. This term is also highly dependent on the geometry and loading condition as T , Q and h are. The relative magnitude of this term compared to the first term in the series is proportional to the parameter L , defined as:

$$L = \frac{1}{G} \left. \frac{\partial G}{\partial s} \right|_P \quad (16)$$

where G is the energy release rate and ∂s represents an extension of the crack along the normal to the crack front. Work is under way to explore the possibility of using this parameter as the second one to describe crack-tip fields and to attempt to connect L with those parameters mentioned above.

Preliminary results are shown in Figs. 8-10. Plots of L vs ϕ are shown for different a/c and a/t values. As it can be seen, for the case of $a/c = 0.6$ and 2 the special feature of a maximum (minimum) occurs at an intermediate angle. This fact has been reported by some authors in terms of the other constraint parameters.

4. DATA GENERATION

Task 4 of this program consists of the generation of R -Curve for materials other than 2219 Al.

It was decided to use 21-6-9 Stainless Steel provided by MM. The test matrix appears in Table 3.

R-Curves for side grooved and non-side grooved specimens are shown in Figs. 11-13. It can be seen that both curves show the same slope of about $dJ/da = 20,000$ psi. On the other hand, the value of J at the point of departure from the blunting line is almost two times larger in the case of the non-side grooved specimens compared to that for the side grooved one. This seems to indicate that the variation in resistance to crack growth with constraint is appreciable.

The rest of the experimental program is under way.

5. CONCLUSIONS

In this report the progress made to date in this project, after six months of performance, is presented.

Task 1: Analytical Studies

A critical review of the existent literature has been performed

Important findings are shown: A method is presented to obtain values of J as a function of position along the crack front based on existing linear elastic solutions and $P-v_{pl}$ calibration curves needed for the specific material/geometry combination.

Task 2: Characterization of Constraint

Candidate parameters were identified. Their implementation for our cases of interest is under way.

A new parameter based on the crack opening displacement profile is being considered. Preliminary results are shown.

Task 4: Data Generation

R-Curve data are being generated on a 21-6-9 Stainless Steel provided by MM. Preliminary results from CT specimens seem to show appreciable material susceptibility to constraint.

Task 3 and 5

They will be started in the near future, when the other tasks are close to completion.

6. REFERENCES

1. McCabe, D. E., "Flaw growth Analysis for 2219-T87 Aluminum Pressure Vessel Welds", Final Report, Contract No. A71257, Martin Marietta Aerospace, New Orleans, November 1988.
2. McCabe, D. E., "Predictive Methodology for Integrity of Tank Welds with Crack-like Defects", Interim Report, Contract No. A71340, Martin Marietta Aerospace, New Orleans, November 1989.
3. McCabe, D. E., Ernst, H. A., and Newman, J. C., "Application of Elastic and Elastic Plastic Fracture Mechanics Methods to Surface Flaws", presented at the XXII National Symposium on Fracture Mechanics, Atlanta, GA, June 1990.
4. Ernst, H.A. "Analysis of Surface Cracks", Final Report, Martin Marietta SC-273183, May 1991.
5. Rice, J. R., Journal of Applied Mechanics, Vol. 35, 1968, pp. 379-386.
6. Sumpter, J. D. G., and Turner, C. E., "Method for Laboratory Determination of J_c ", Cracks and Fracture, ASTM STP 601, American Society for Testing and Materials, 1976, pp. 3-18.
7. Ernst, H. A., Paris, P. C., Rossow, M., and Hutchinson J. W., in "Fracture Mechanics", ASTM STP 677, American Society for Testing and Materials", 1979, pp. 581-599.
8. Dodds, R. H., and Kirk, M. T. Civil Engineering Studies, SRS 353, Univ. of Illinois, July 1989.
9. McClung, R. C., et al, "Growth of Cracks During Large Elastic-Plastic Loading Cycles", XXIII National Symposium on Fracture Mechanics, TX, 1991.
10. Newman, J. C., and Raju, I.S., "Stress intensity Factor Equations for cracks in Three Dimensional Finite Bodies," ASTM STP 791, American Society for Testing and Materials, 1983, pp. I-238-265.
11. Bertegon, C. and Hancock, J. W. "Two Parameter Characterization of Elastic Plastic Crack Tip Fields", Journal of Applied Mechanics, 1990.
12. O'Dowd, N. P. and Shih, C. F. Family of Crack Tip Fields Chracterized by a Triaxiality Parameter: Part I and II", J. of Mechanics and Physics of Solids, 1991.
13. Brocks. W. and Kunecke, G., In Proc. 14th MPA Seminar, Stuuatgart, 1988.
14. Tada, H., Paris, P. C. and Irwin, G. R., "The Stress Analysis of Cracks Handbook", Del Research Corp. St. Louis, Mo, 1976

7. TABLES

TABLE 1

Average Normalized G Values

a/c	a/t	G _N ave
0.6	0.35	0.753
0.6	0.55	1.393
0.6	0.75	2.251
1.0	0.35	0.538
1.0	0.55	0.918
1.0	0.75	1.372
2.0	0.35	0.085
2.0	0.55	0.136
2.0	0.75	0.191

$$G_N \text{ ave} = \frac{2}{\pi} \int_0^{\pi/2} (GEt/\sigma^2) d\phi \quad t = 0.5"$$

$$E = 10.52 \cdot 10^3 \text{ ksi}$$

TABLE 2***Coefficient D for different a/c and a/t***

a/c	a/t	D(inch ⁻¹)
0.6	0.35	5.7866x10 ⁻¹⁰
0.6	0.55	1.7872x10 ⁻¹⁰
0.6	0.75	0.7535x10 ⁻¹⁰
1.0	0.35	10.618x10 ⁻¹⁰
1.0	0.55	3.5565x10 ⁻¹⁰
1.0	0.75	1.621x10 ⁻¹⁰
2.0	0.35	97.463x10 ⁻¹⁰
2.0	0.55	34.635x10 ⁻¹⁰
2.0	0.75	16.787x10 ⁻¹⁰

TABLE 3**Test Matrix****SCT Specimens**

Number of Specimens	a_o	$2c_o$	a/c	a/t
3	0.05"	0.05"	2	0.2
1	0.10"	0.10"	2	0.4
3	0.15"	0.15"	2	0.6
1	0.05"	0.10"	1	0.2
3	0.10"	0.20"	1	0.4
1	0.15"	0.30"	1	0.6
3	0.05"	0.167"	0.6	0.2
3	0.10"	0.33"	0.6	0.4
3	0.15"	0.50"	0.6	0.6

CT Specimens: Different a/w , Side-Grooved and Non Side-Grooved

CCT Parameters: Different a/u , Side-Grooved and Non Side-Grooved

8. FIGURES

1. Geometry of elliptical crack
2. Normalized G vs Angle $a/c = 0.6$
3. Normalized G vs Angle $a/c = 1.0$
4. Normalized G vs Angle $a/c = 2.0$
5. Total J vs Angle, different load levels, $a/c = 0.6$, $a/t = 0.35$
6. Total J vs Angle, different load levels, $a/c = 0.6$, $a/t = 0.55$
7. Total J vs Angle, different load levels, $a/c = 0.6$, $a/t = 0.75$
8. Total J vs Angle, different load levels, $a/c = 1.0$, $a/t = 0.35$
9. Total J vs Angle, different load levels, $a/c = 1.0$, $a/t = 0.55$
10. Total J vs Angle, different load levels, $a/c = 1.0$, $a/t = 0.75$
11. Total J vs Angle, different load levels, $a/c = 2.0$, $a/t = 0.35$
12. Total J vs Angle, different load levels, $a/c = 2.0$, $a/t = 0.55$
13. Total J vs Angle, different load levels, $a/c = 2.0$, $a/t = 0.75$
14. Measure of Constraint vs Angle, $a/c = 0.6$
15. Measure of Constraint vs Angle, $a/c = 1.0$
16. Measure of Constraint vs Angle, $a/c = 2.0$
17. J- R Curve for Non-side grooved CT specimens
18. J- R Curve for Side grooved CT specimens
19. J- R Curve for CT specimens

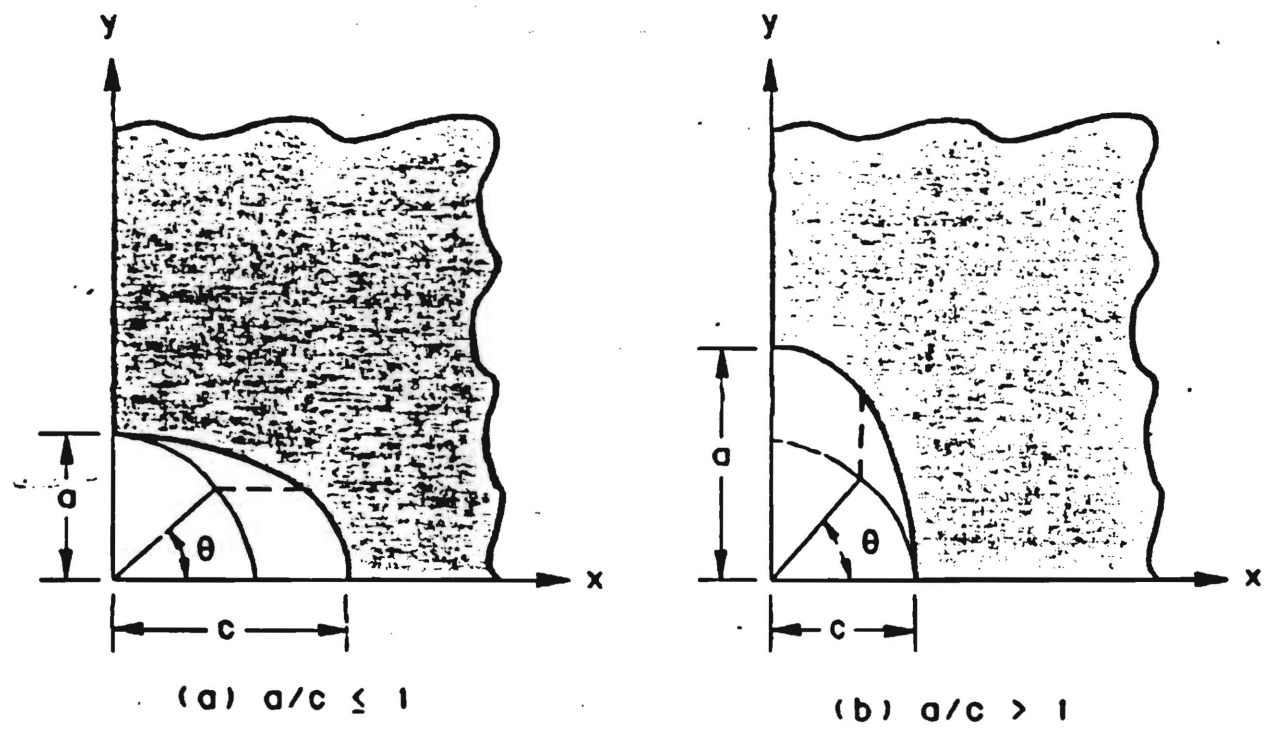


Fig. 1 Geometry of elliptical crack

Normalized G

$\alpha/c = 0.6$ $t = 0.5''$

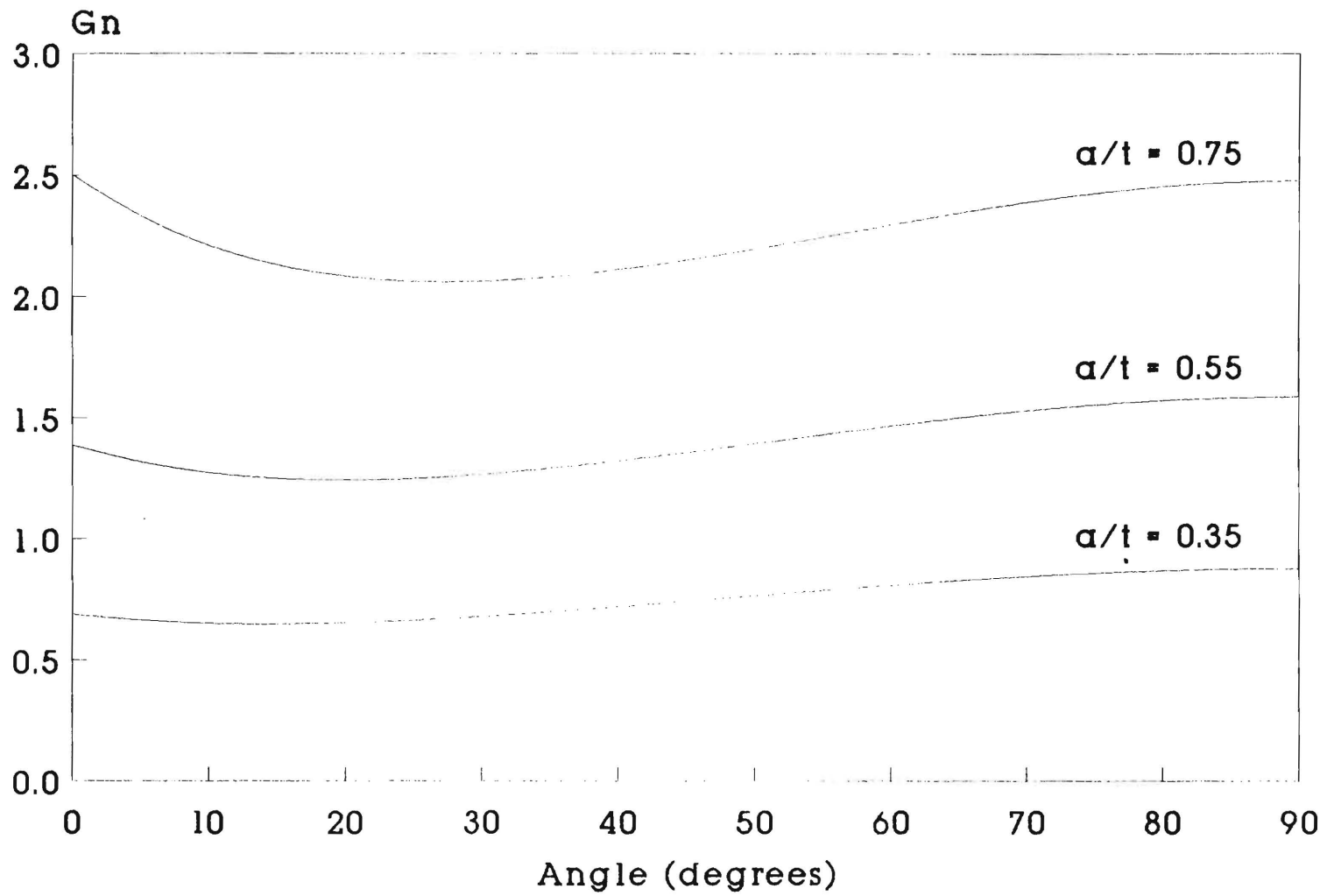


Fig. 2 Normalized G vs Angle

Normalized G

$a/c = 1.0 \quad t = 0.5''$

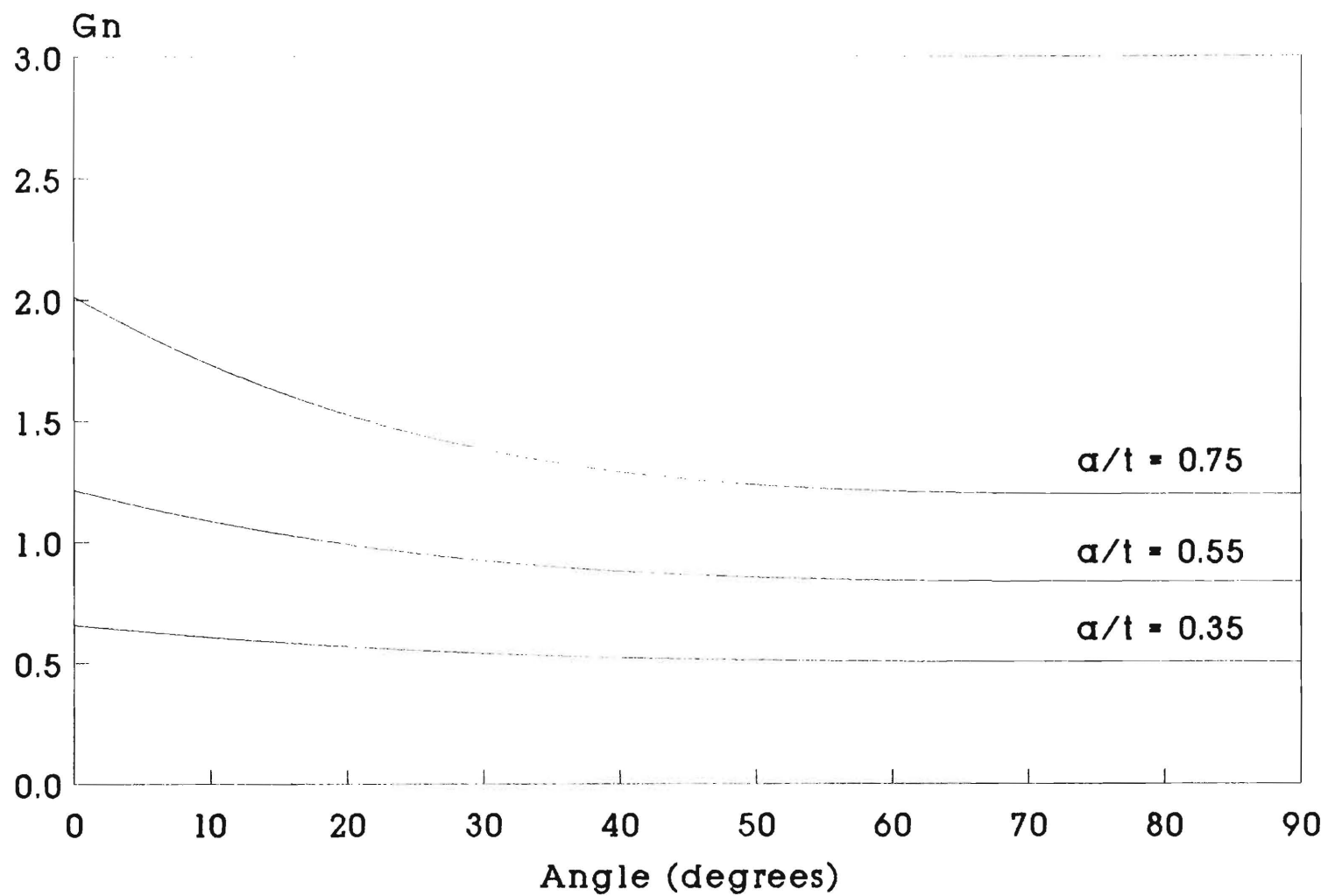


Fig. 3 Normalized G vs Angle

Normalized G

$a/c = 2.0 \quad t = 0.5"$

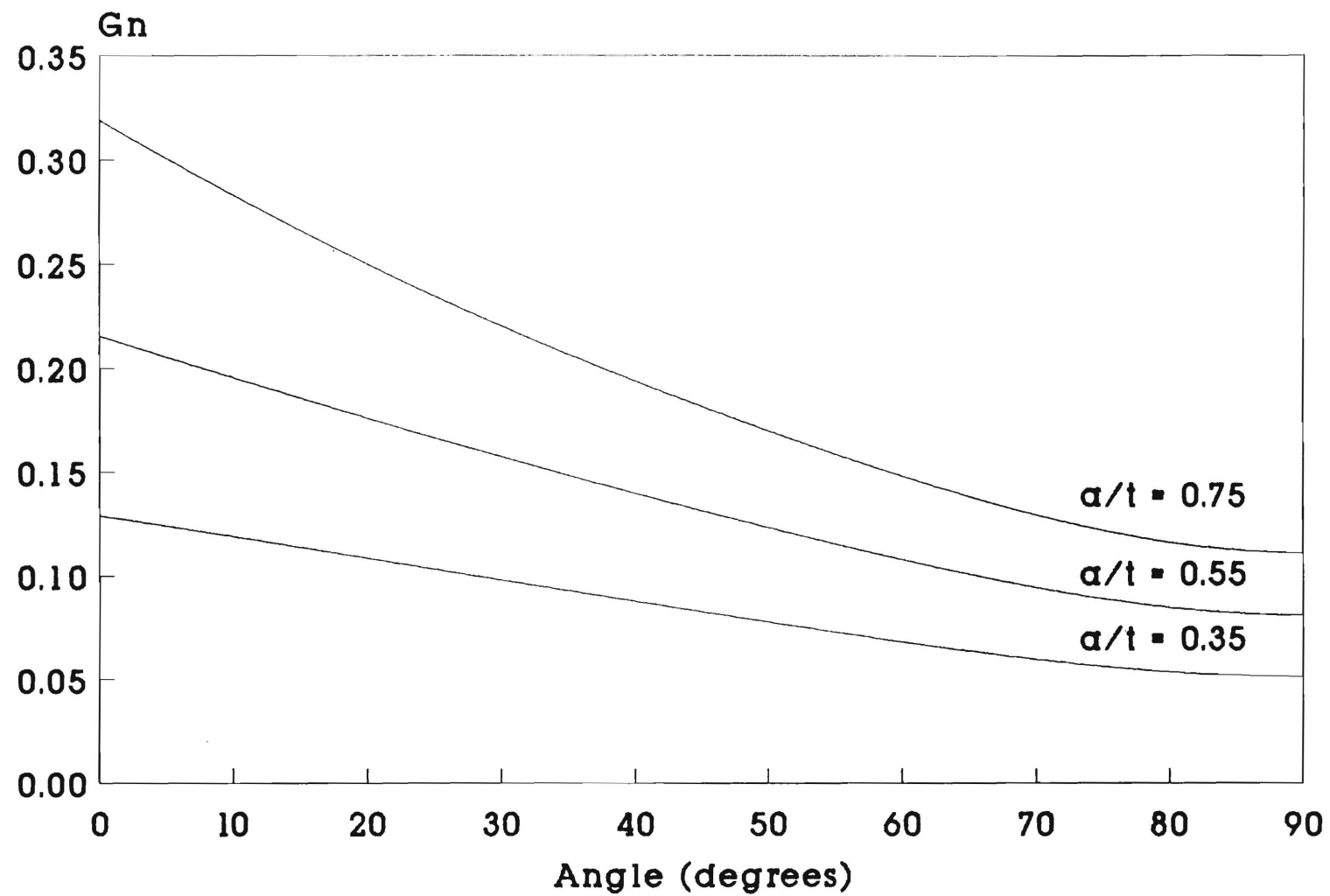


Fig. 4 Normalized G vs Angle

Local J-Integral Calculations

$a/c=0.6$ $a/t=0.35$ $t=0.5"$

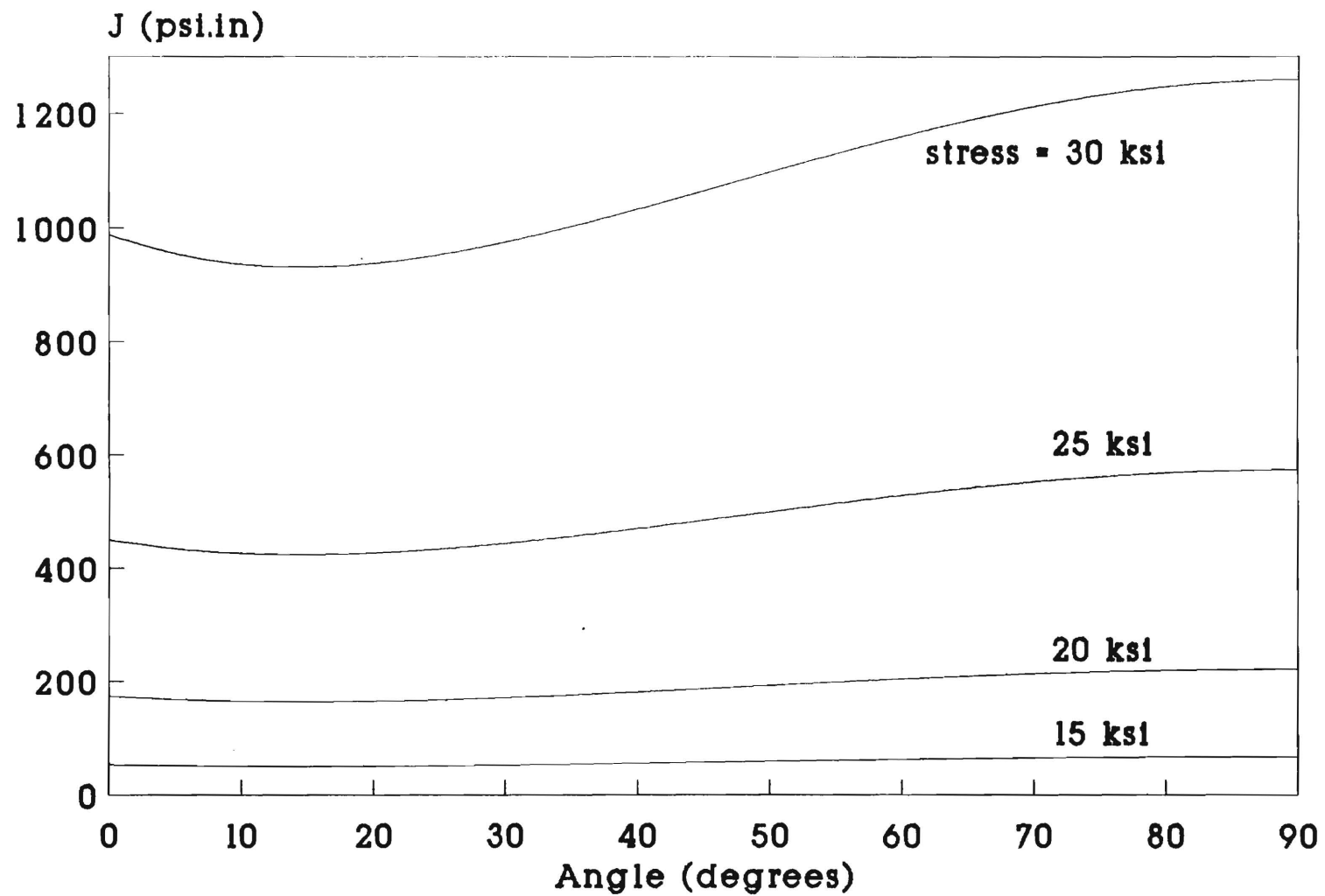


Fig. 5 J vs Angle

Local J-Integral Calculations

$a/c=0.6$ $a/t=0.55$ $t=0.5"$

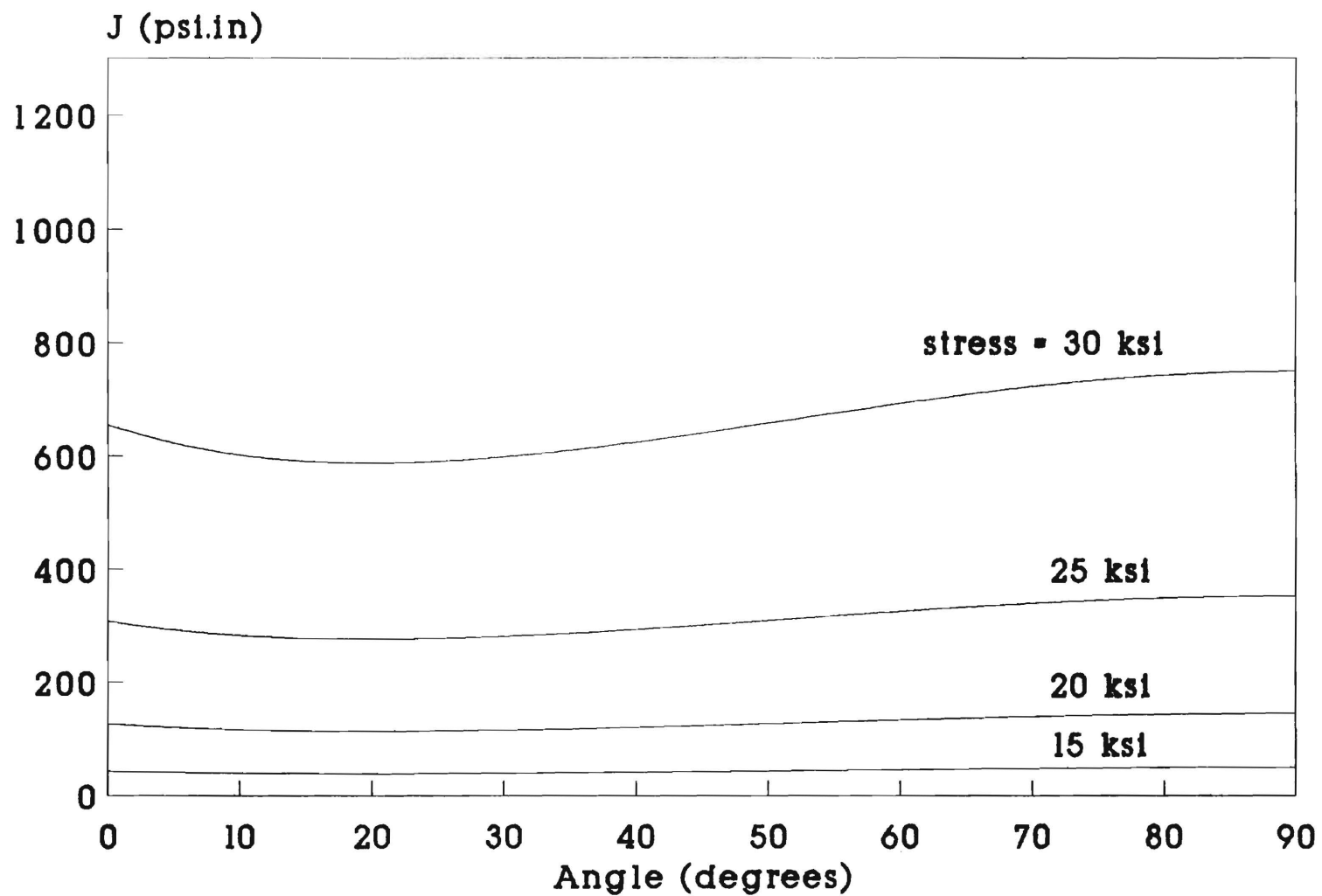


Fig. 6 J vs Angle

Local J-Integral Calculations

$a/c=0.6$ $a/t=0.75$ $t=0.5"$

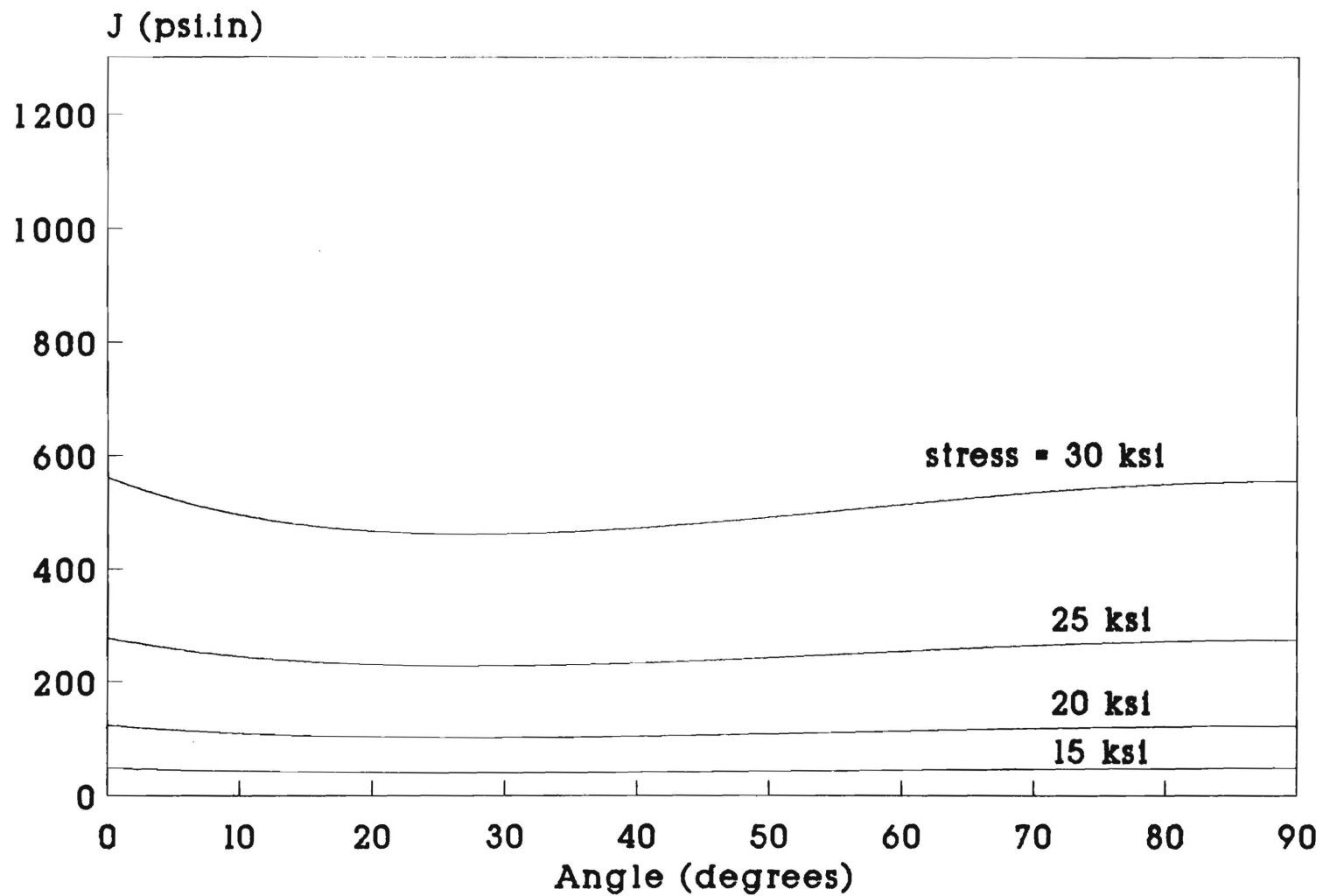


Fig. 7 J vs Angle

Local J-Integral Calculations

$a/c=1.0$ $a/t=0.35$ $t=0.5"$

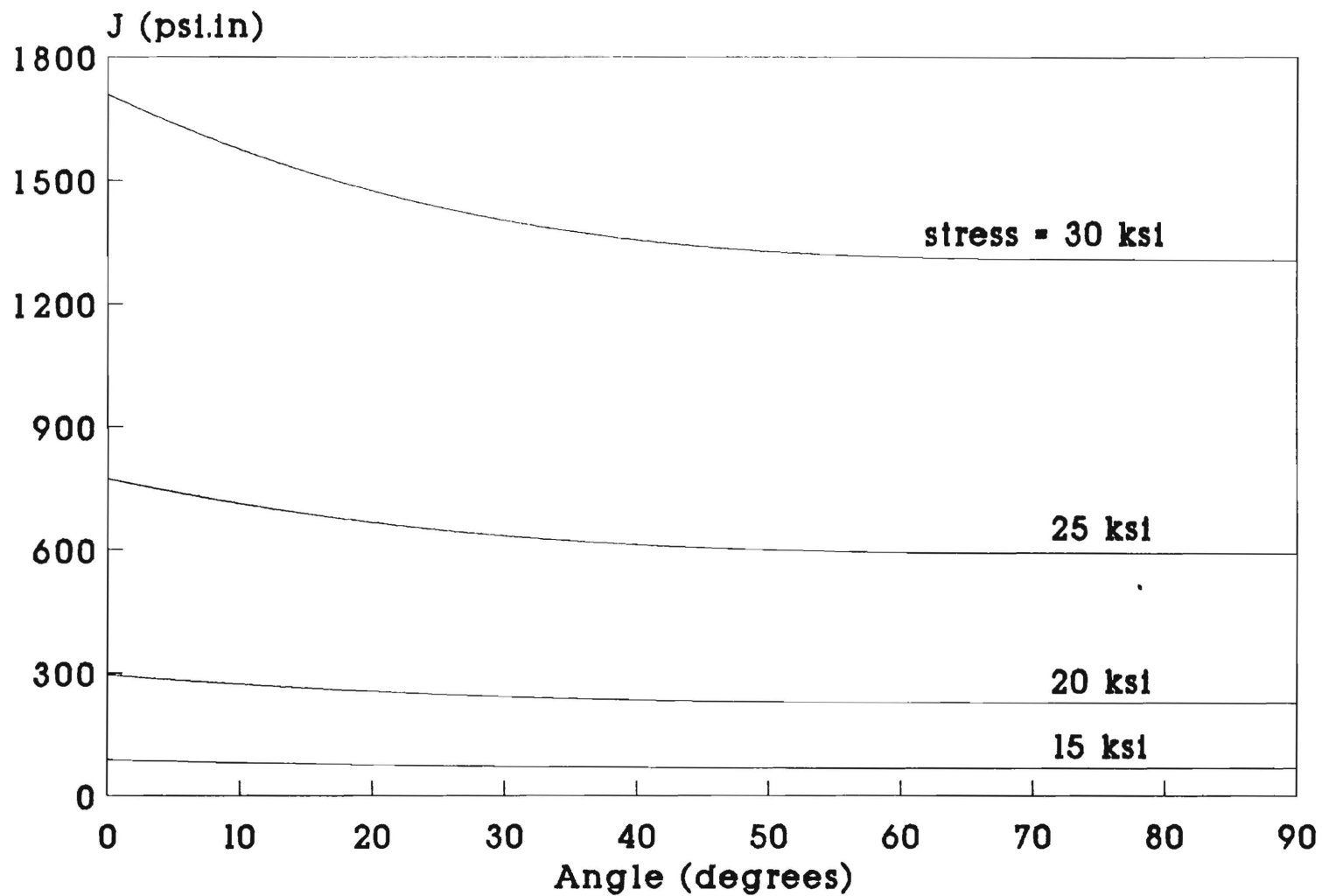


Fig. 8 J vs Angle

Local J-Integral Calculations

$a/c=1.0$ $a/t=0.55$ $t=0.5"$

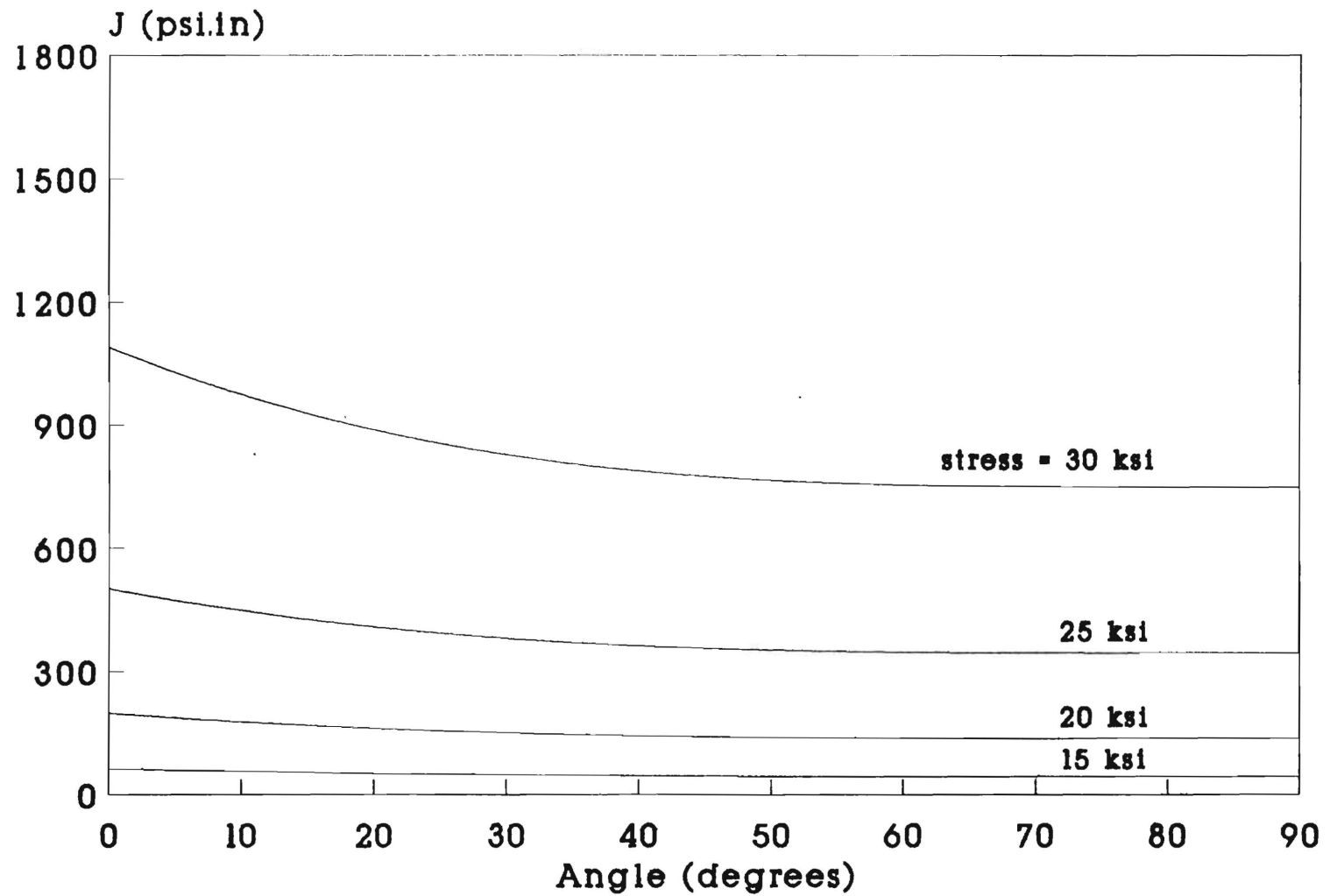


Fig. 9 J vs Angle

Local J-Integral Calculations

$a/c=1.0$ $a/t=0.75$ $t=0.5"$

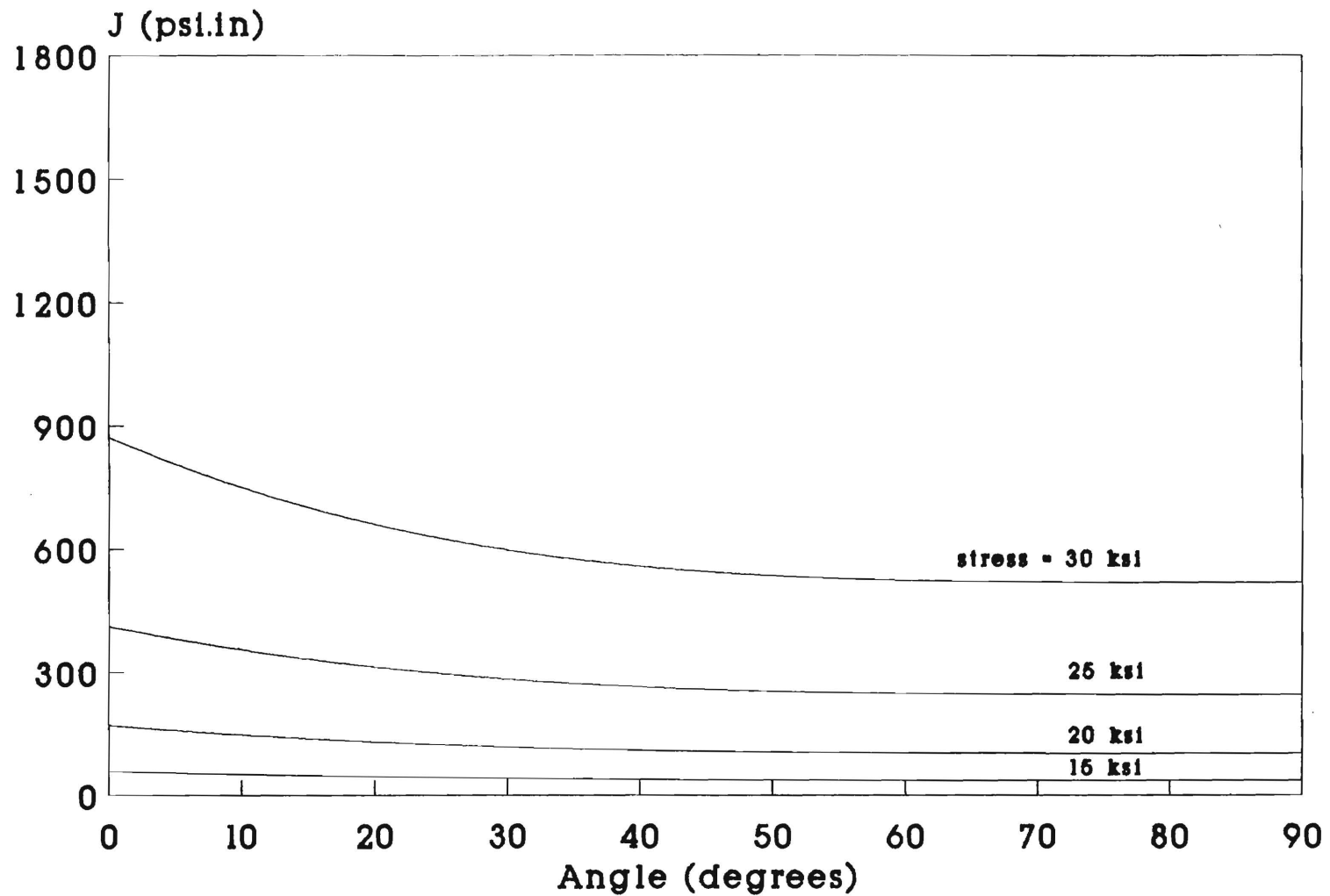


Fig. 10 J vs Angle

Local J-Integral Calculations

$\alpha/c=2.0$ $\alpha/t=0.35$ $t=0.5"$

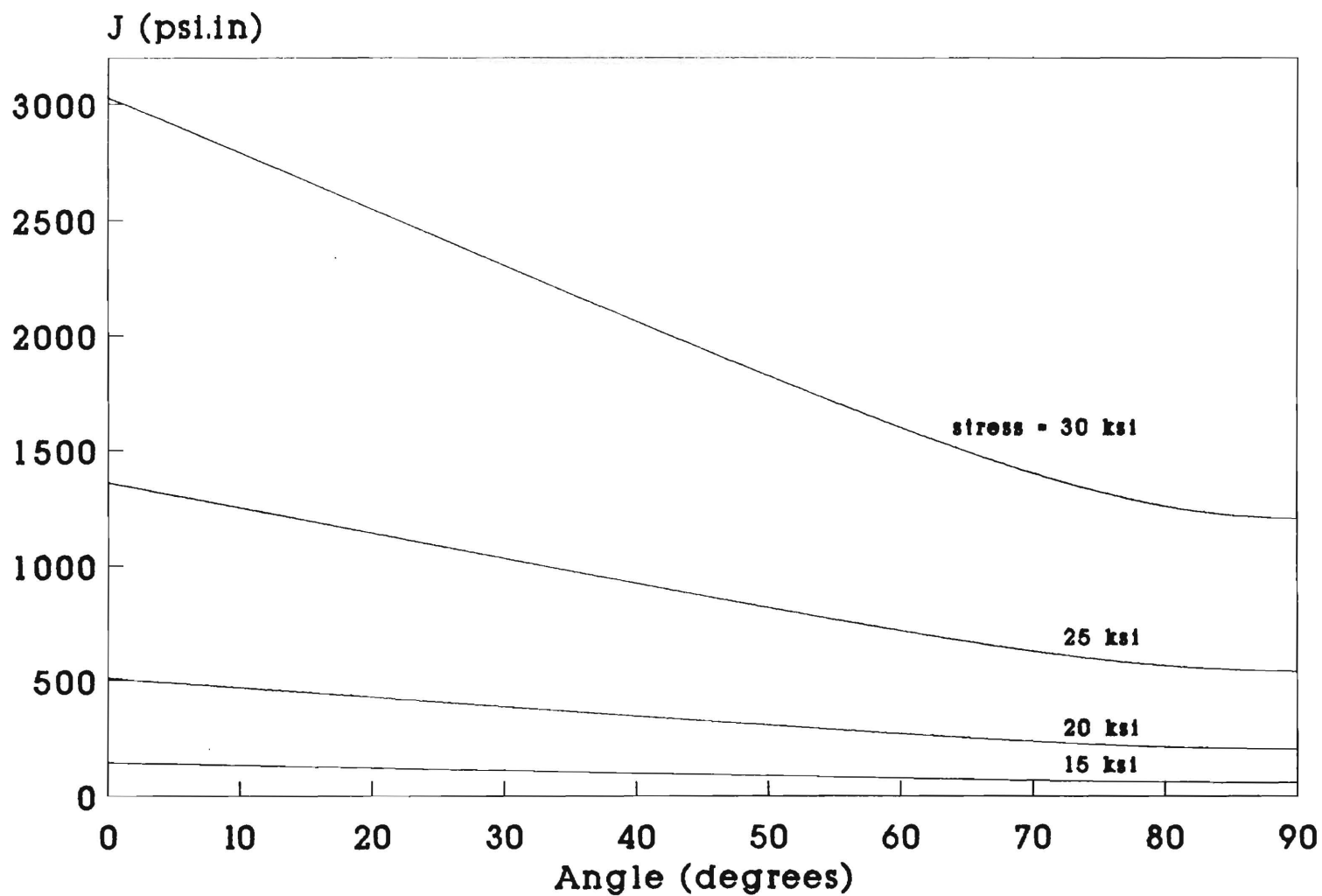


Fig. 11 J vs Angle

Local J-Integral Calculations

$a/c=2.0$ $a/t=0.55$ $t=0.5"$

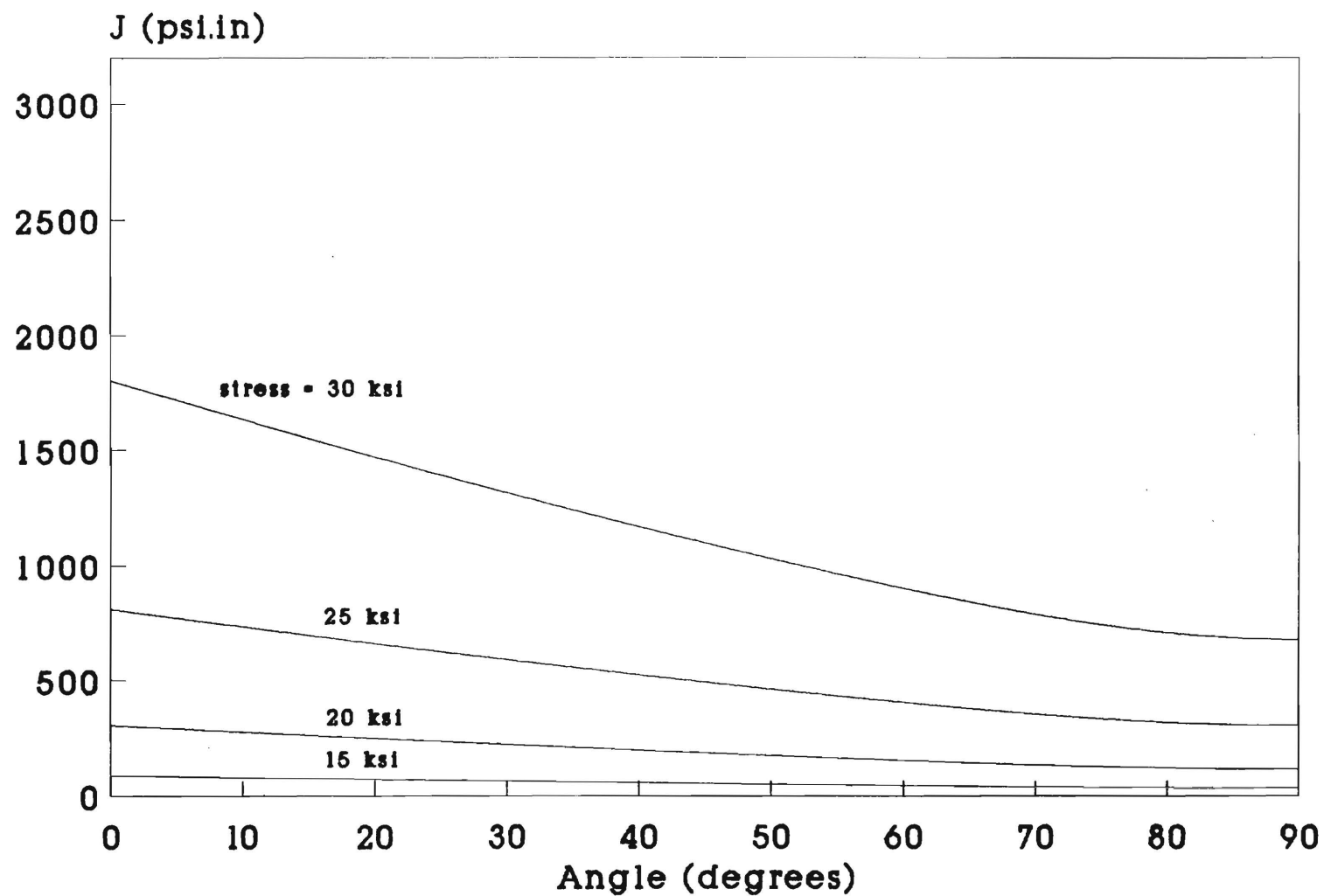


Fig. 12 J vs Angle

Local J-Integral Calculations

$a/c=2.0$ $a/t=0.75$ $t=0.5"$

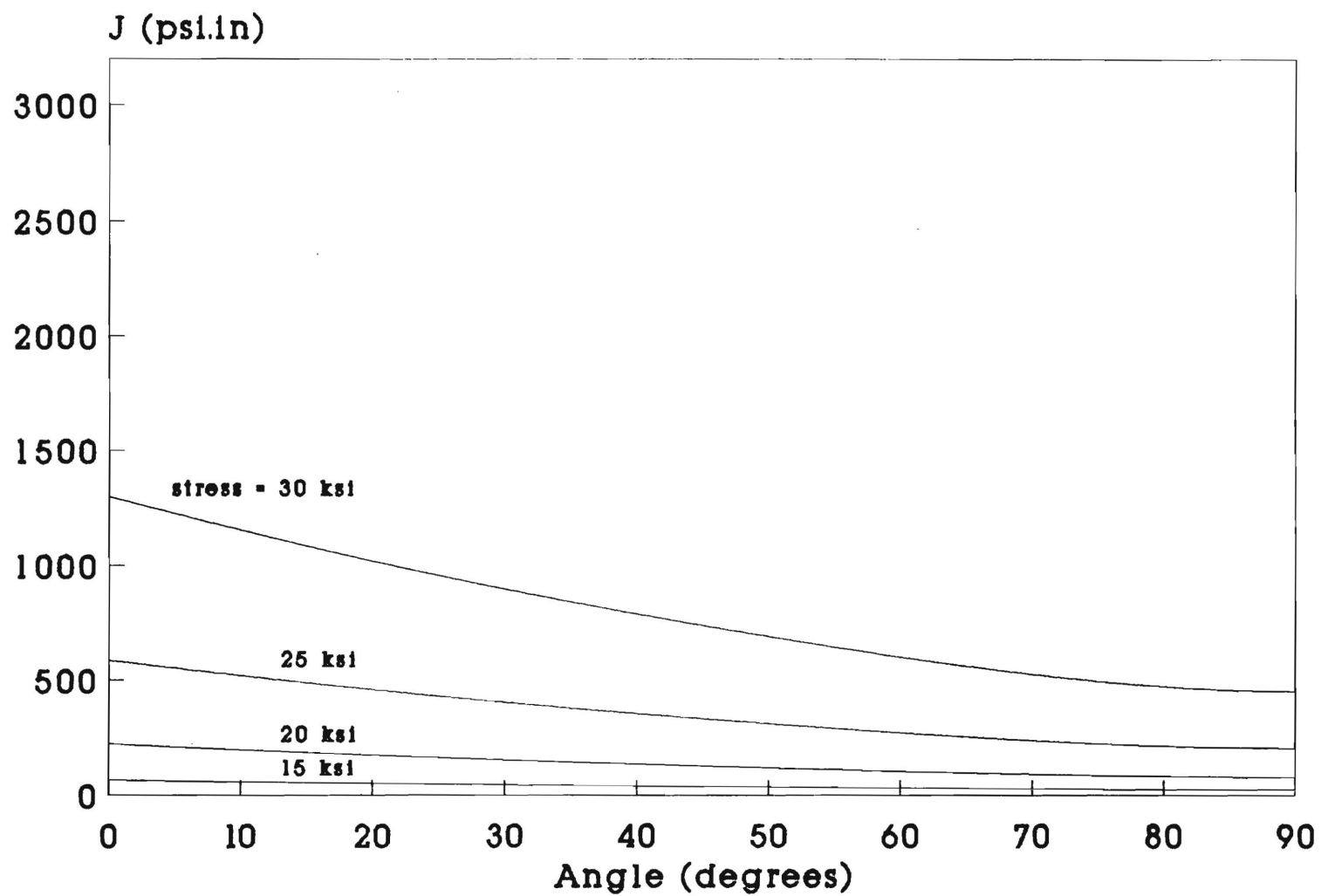


Fig. 13 J vs Angle

Measure of Constraint vs. Angle

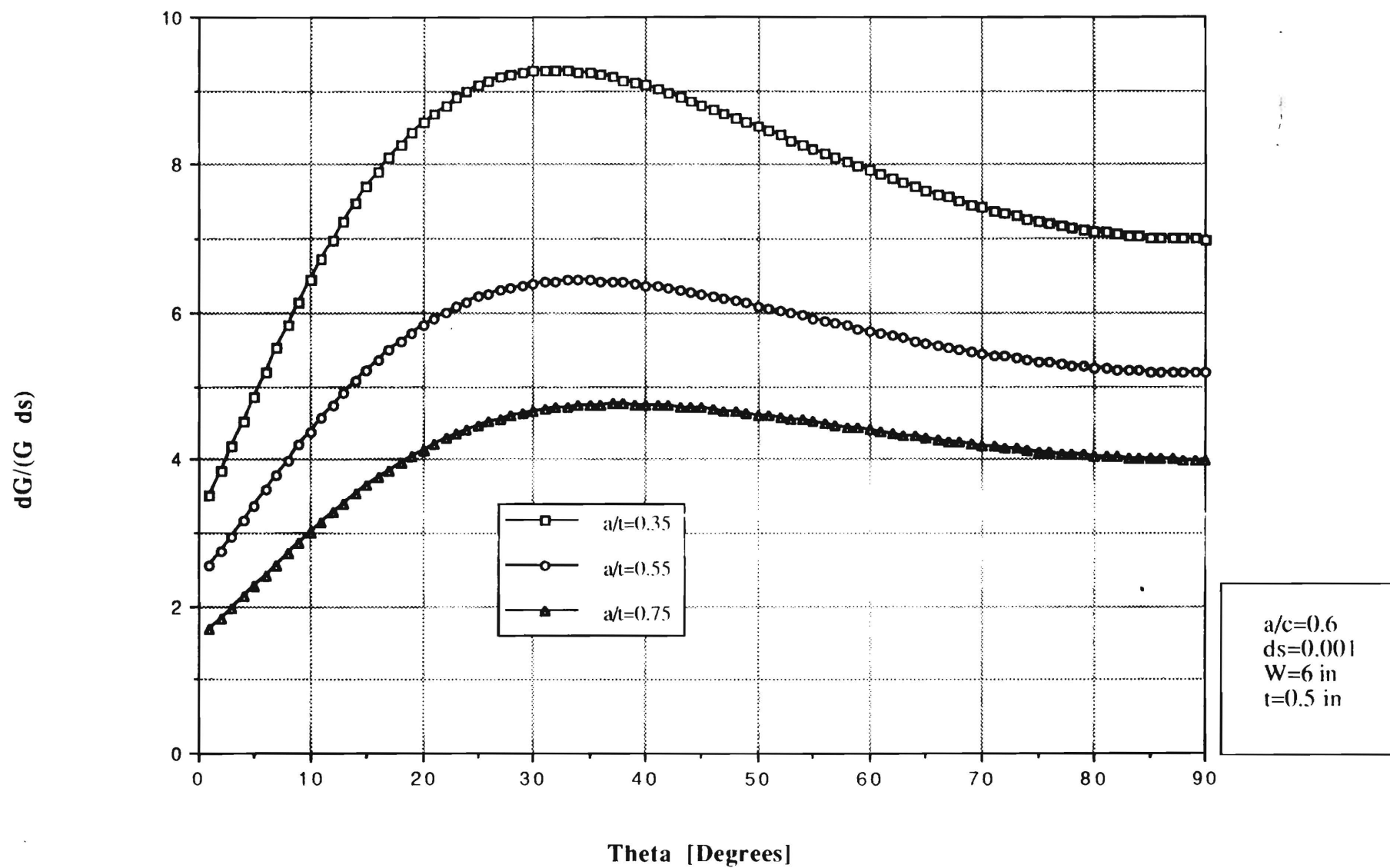


Fig. 14 Measure of Constraint vs Angle

Measure of Constraint vs. Angle

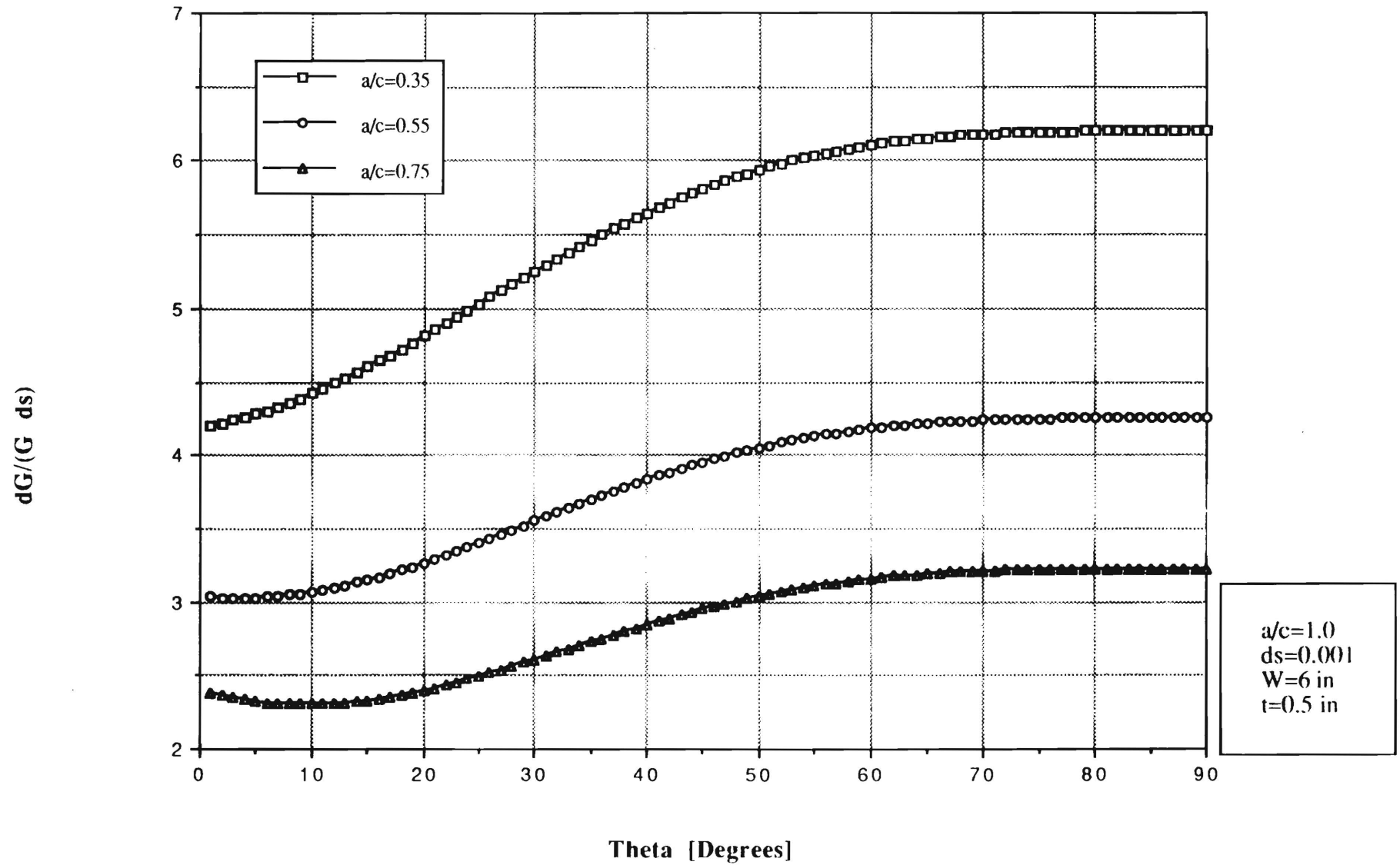


Fig. 15 Measure of Constraint vs Angle

Measure of Constraint vs. Angle

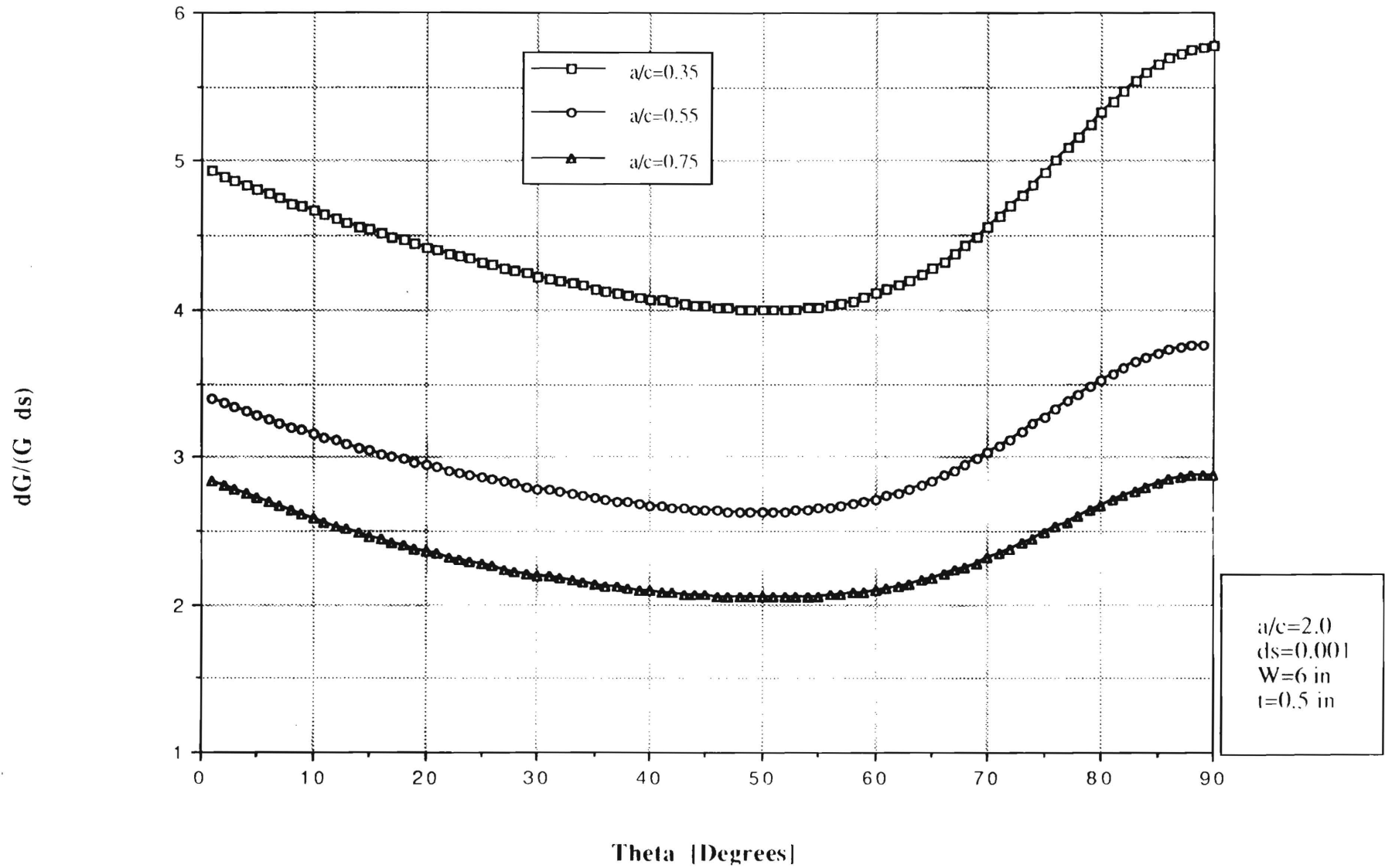


Fig. 16 Measure of Constraint vs Angle

J-R Curve for 21-6-9 SS Non Side-Grooved

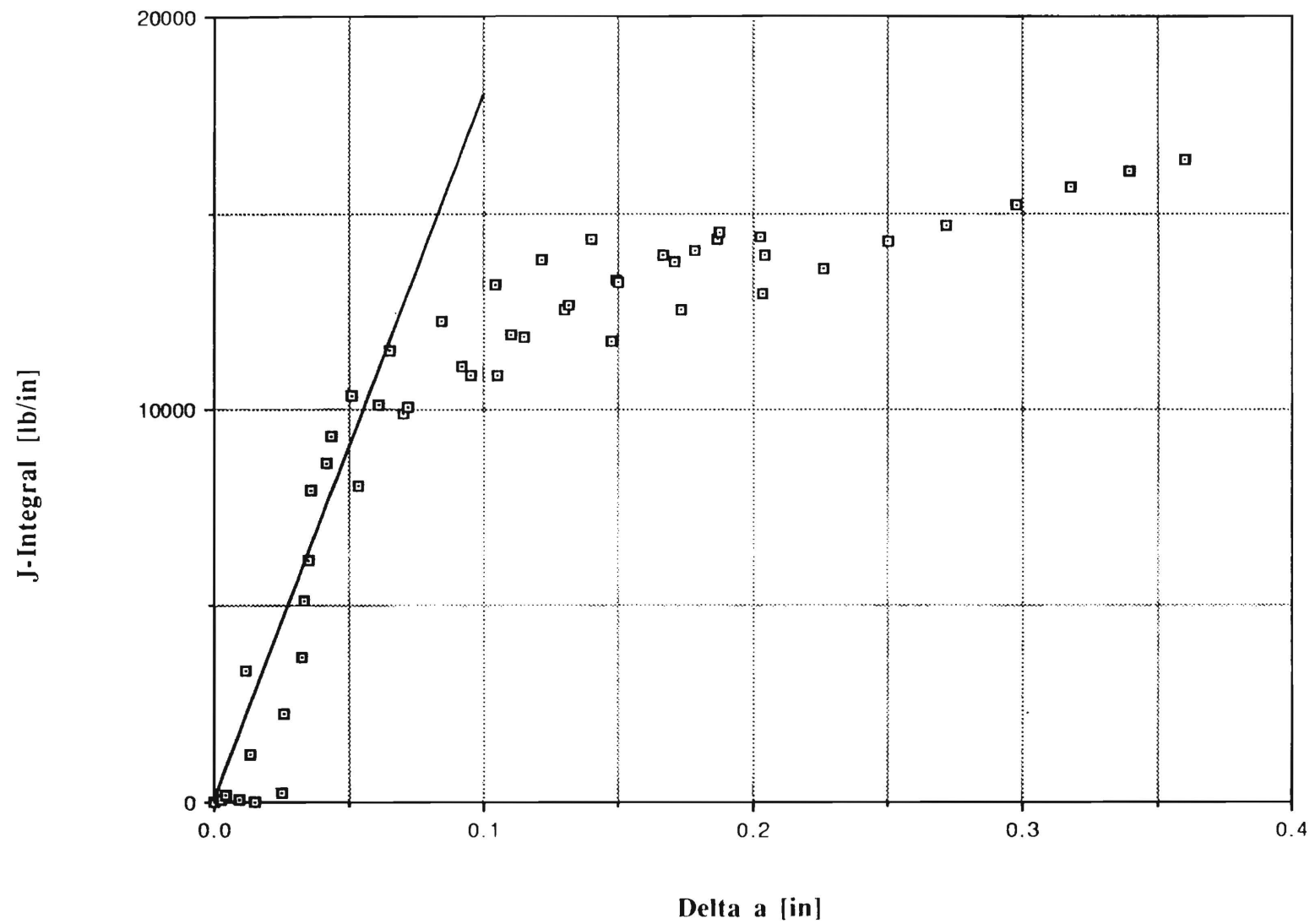


Fig. 17 J-R Curve for Non side-grooved CT specimens

J-R Curve for 21-6-9 SS Side Grooved

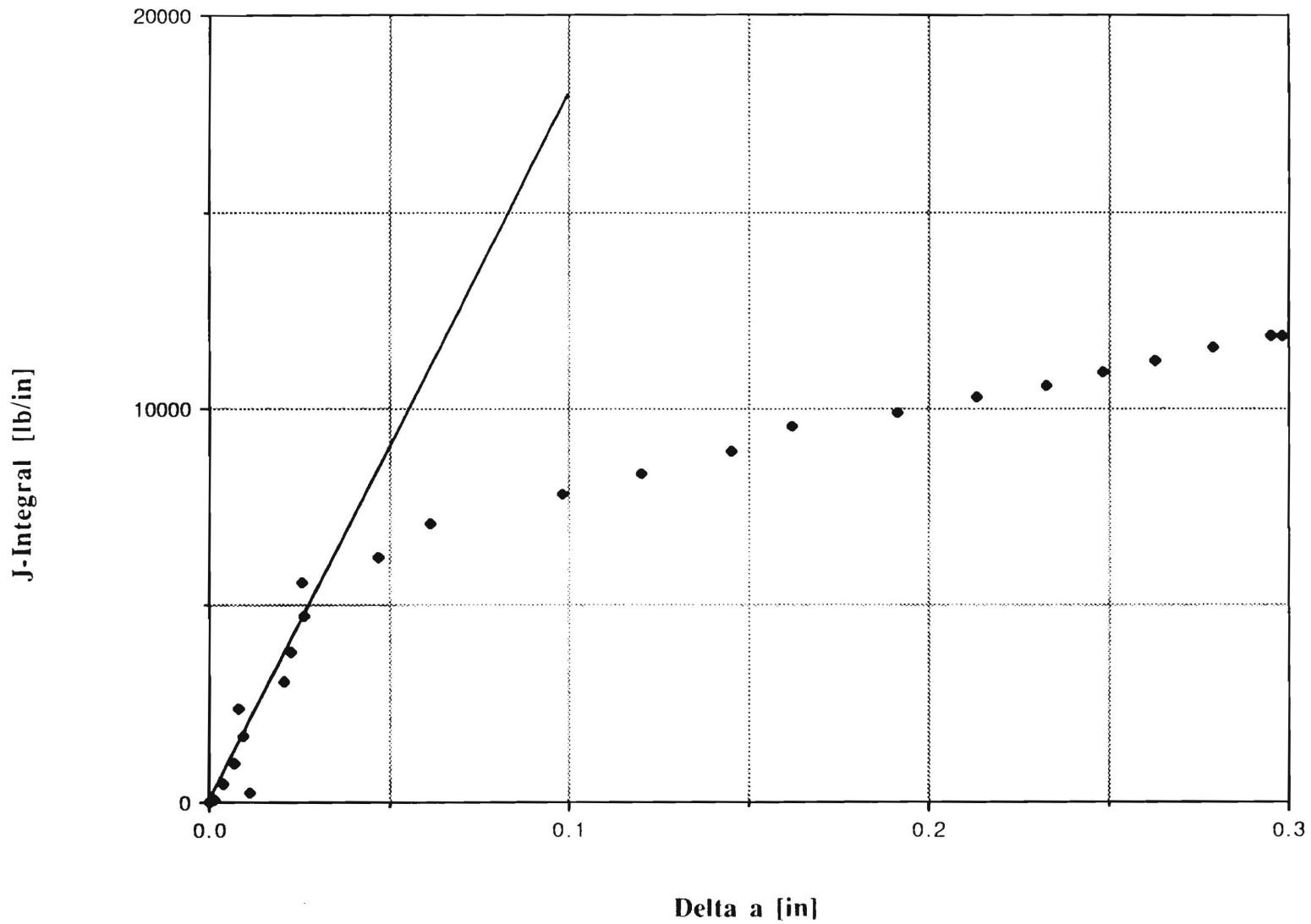


Fig. 18 J-R Curve for Side-grooved CT specimens

J-R Curve for 21-6-9 SS

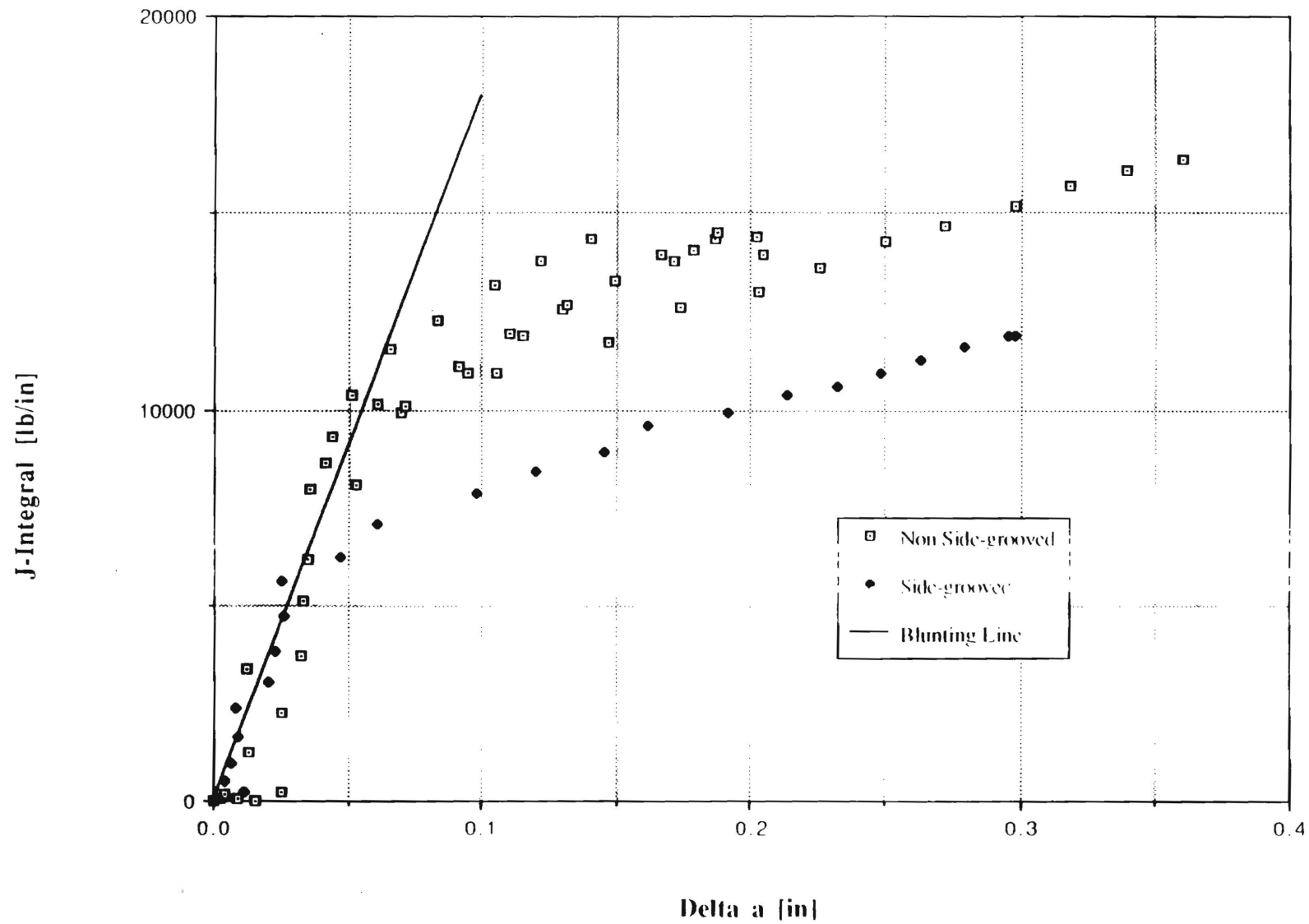


Fig. 19 J Resistance Curve All CT Specimens